Mineralogical Magazine, October 2008, Vol. 72(5), pp. 1083–1101

Coiraite, $(Pb,Sn^{2+})_{12.5}As_3Fe^{2+}Sn_5^{4+}S_{28}$: a franckeite-type new mineral species from Jujuy Province, NW Argentina

W. H. Paar[1,*], Y. Moëlo[2], N. N. Mozgova[3], N. I. Organova[3], C. J. Stanley[4], A. C. Roberts[5], F. J. Culetto[6], H. S. Effenberger[7], D. Topa[1], H. Putz[1], R. J. Sureda[8] and M. K. de Brodtkorb[9]

[1] Department of Materials Engineering and Physics (Division of Mineralogy), University of Salzburg, Hellbrunnerstr. 34, A-5020 Salzburg, Austria
[2] Institut des Matériaux J.Rouxel (IMN), Université de Nantes, CNRS, 2, rue de la Houssinière, F-44322 Nantes Cedex 3, France
[3] IGEM RAS, Staromonetny 35, Moscow, 119017, Russia
[4] The Natural History Museum, Cromwell Road, London, SW7 5BD, England, UK
[5] Geological Survey of Canada, 601 Booth Street, Ottawa, Ontario K1A OE8, Canada
[6] KELAG-Kärntner Elektrizitäts-Aktiengesellschaft, Arnulfplatz 2, A-9020 Klagenfurt, Austria
[7] Institut für Mineralogie und Kristallographie, Universität Wien, Althanstrasse 14, A-1090 Vienna, Austria
[8] Cátedra de Mineralogía, Facultad de Ciencias Naturales, Universidad Nacional de Salta, 4400 Salta, Argentina
[9] Consejo Nacional de Investigaciones Científicas y Técnicas, Universidad de Buenos Aires, Paso 258-9º, 1640 Martinez, Argentina

[*Received 11 August 2008; Accepted 13 January 2009*]

ABSTRACT

Coiraite, ideally $(Pb,Sn^{2+})_{12.5}As_3Fe^{2+}Sn_5^{4+}S_{28}$, occurs as an economically important tin ore in the large Ag-Sn-Zn polymetallic Pirquitas deposit, Jujuy Province, NW-Argentina. The new mineral species is the As derivative of franckeite and belongs to the cylindrite group of complex Pb sulphosalts with incommensurate composite-layered structures. It is a primary mineral, frequently found in colloform textures, and formed from hydrothermal solutions at low temperature. Associated minerals are franckeite, cylindrite, pyrite-marcasite, as well as minor amounts of hocartite, Ag-rich rhodostannite, arsenopyrite and galena. Laminae of coiraite consist of extremely thin bent platy crystals up to 50 μm long. Electron microprobe analysis (n = 31) gave an empirical formula $Pb_{11.21}As_{2.99}Ag_{0.13}Fe_{1.10}Sn_{6.13}S_{28.0}$, close to the ideal formula $(Pb_{11.3}Sn^{2+}_{1.2})_{\Sigma=12.5}As_3Fe^{2+}Sn_5^{4+}S_{28}$. Coiraite has two monoclinic sub-cells, Q (pseudotetragonal) and H (pseudohexagonal). Q: a 5.84(1) Å, b 5.86(1) Å, c 17.32(1) Å, β 94.14(1)º, V 590.05(3) Å^3, Z = 4, $a:b:c$ = 0.997:1:2.955; H (orthogonal setting): a 6.28(1) Å, b 3.66(1) Å, c 17.33(1) Å, β 91.46(1)º, V 398.01(6) Å^3, Z = 2, $a:b:c$ = 1.716:1:4.735. The strongest Debye-Scherrer camera X-ray powder-diffraction lines [d in Å, (I), (hkl)] are: 5.78, (20), (Q and H 003); 4.34, (40), (Q 004); 3.46, (30), (Q and H 005); 3.339, (20), (Q 104); 2.876, (100), (Q and H 006); 2.068, (60), (Q 220).

Keywords: coiraite, As-derivative of franckeite, tin, arsenic, cylindrite group, sulphosalt.

Introduction

In 1997, one of us (MKdB) gave to the senior author several unnamed mineral species from the Pirquitas deposit, Jujuy Province, NW Argentina. The samples originated from a major exploration project at this location although the exact locations of the samples in the abandoned mine are not known. Several years later, detailed mapping by the first author was undertaken in the Oploca sector of this deposit. In one of the drifts, a vein was exposed which was initially named 'suredaite vein' (Paar *et al.*, 2000) and subsequently 'Veta Oploca Norte', the 'northern

* E-mail: werner.paar@sbg.ac.at
DOI: 10.1180/minmag.2008.072.5.1083

Oploca vein' (Paar *et al.*, 2001). This vein attracted our interest because of a well developed banded texture with mineralogy very similar to that of the hand specimens obtained in 1997. One of the mineralized bands, almost 2 cm wide, consisted of a phase with a metallic lustre and needle-shaped habit. This phase was characterized as the new mineral species suredaite, $PbSnS_3$ (Paar *et al.*, 2000).

Other bands within the same vein, in close association with suredaite, consisted of an inconspicuous grey to dark grey, microcrystalline mineral, which closely resembled an oxidized manganese species. Preliminary analysis by electron microprobe indicated Pb, Sn, As, Fe and S as the major elements, and X-ray powder-diffraction patterns suggested a relation with a franckeite-type sulphosalt. In two papers by Paar *et al.* (2000, 2001), this phase was mentioned as "As-rich franckeite" and "As-franckeita", respectively. In subsequent characterization of this new mineral species, numerous attempts were made to obtain unit-cell parameters by single-crystal X-ray diffraction, but without success due to the very fine-grained and intergrown nature of the available material.

The new mineral species reported here has been approved by the CNMNC of the IMA (proposal 2005-24). It is named after Beatriz Lydia Coira (born 1941), Professor of Petrology at the University of Jujuy, NW Argentina, for her outstanding research on volcanism, regional geology and its relation to ore-deposit formation in Argentina.

Several specimens showing the typical association of coiraite and suredaite are deposited in the mineralogical collections at: the Department of Materials Engineering and Physics, University of Salzburg, Austria, registered under catalogue numbers 14943-14946, in the reference collections of the Natural History Museum, London, UK (BM 2008, 47), the Landesmuseum Joanneum, Graz, Styria Province of Austria and in the ore deposit collection of the Chair of Mineralogy ('Cátedra de Mineralogia'), Faculty of Natural Sciences, University of Salta, Argentina.

Location and general geology

The Pirquitas mining district is located in the Puna, 135 km west of Abra Pampa in the Province of Jujuy, NW Argentina at 22º41′S and 66º28′W (Fig. 1). The mineralization is genetically comparable to the epi- and mesothermal systems of the Bolivian Ag-Sn belt (Ahlfeld and Schneider-Scherbina, 1964; Ericksen and Cunningham, 1993; Sillitoe *et al.*, 1998). Pirquitas is the southernmost representative of this economically very important mineral belt. The ore district of Pirquitas includes primary Ag-Sn-Zn mineralization and placer deposits of alluvial tin and gold, which were exploited intermittently from 1936 to 1999. The in-pit

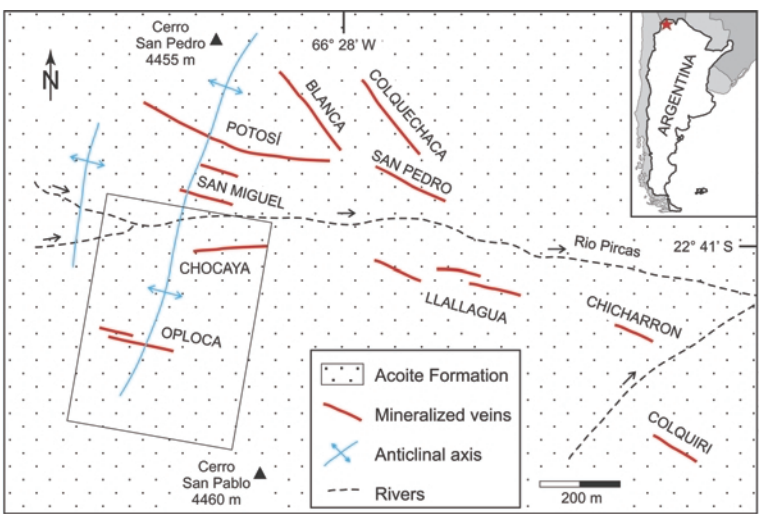

FIG. 1. General geology and major vein systems at Pirquitas, Argentina. The bonanza-grade Ag-Sn mineralization at Oploca is in the SW corner of the district. The black rectangle indicates the sector which is shown in Fig. 2.

proven reserves at Pirquitas (as of 2008) are 10.7 Mt grading 195 ppm Ag, 0.26% Sn and 0.70% Zn, while probable reserves total 19.3 Mt grading 202 ppm Ag, 0.20% Sn and 0.90% Zn. Additional measured, indicated and inferred resources amount to 74.2 Moz, 147 Moz and 18.8 Moz of silver, tin and zinc, respectively. Pirquitas was scheduled to start mining during June 2008, and to produce the first concentrates in April 2009.

The area is underlain by Ordovician sediments of the Acoite Formation which comprise slates, sandstones and greywackes. The dominant veins with economic mineralization (Oploca, Potosi, San Pedro, San Miguel, Llallagua, Chocaya and Colquechaca) trend E–W to WNW–ESE, are subvertical, and were emplaced during the middle and upper Miocene (Coira and de Brodtkorb 1995, Sureda *et al*., 1986) (Fig. 1). All veins become thicker in soft rock and thinner in hard rock. Numerous parallel veins occur between major vein structures, as is particularly notable in the San Miguel sector, the designated 'open-pit zone'.

The intersections of vein structures and axial planes are zones of weakness, where high-grade mineralization typically occurs, particularly at the Oploca vein system (Fig. 1), where a mineralized breccia and cross-cutting high-grade veins were identified (Amann and Paar, 2001; Paar *et al*., 2006*a*,*b*).

The mineralization in all veins at Pirquitas is polymetallic (Malvicini 1978; Paar *et al*., 1996) and was formed in several superimposed pulses, commonly referred to as 'telescoping' in these types of deposits. These multiple hydrothermal pulses precipitated sulphides, sulphosalts and oxides at particularly low temperature, as is indicated by the frequently observed colloform textures of the coiraite-sphalerite-pyrite assemblages.

The Oploca Sector

This economically significant part of the deposit is located in its south-western corner (Figs 1, 2). High-grade Ag-Sn-Zn mineralization occurs as a series of parallel, WNW–ESE trending extensional veins and veinlets in the hinge zone of the Cerro San Pedro anticlinal structure (Figs 1, 2). Principal vein systems, as exposed in the Oploca crosscut (veins Oploca N and Oploca S), and several unnamed veins and veinlets contribute to the ore potential of this sector. The major veins Oploca N and S can be traced underground from their outcrops slightly above level 6 (at 4370 m above sea level) *via* levels 7¼ and 8 downward to level 9¼, which is the Oploca crosscut (at 4250 m above sea level) (Fig. 2).

The veins in this sector show all the characteristics of open space filling, such as

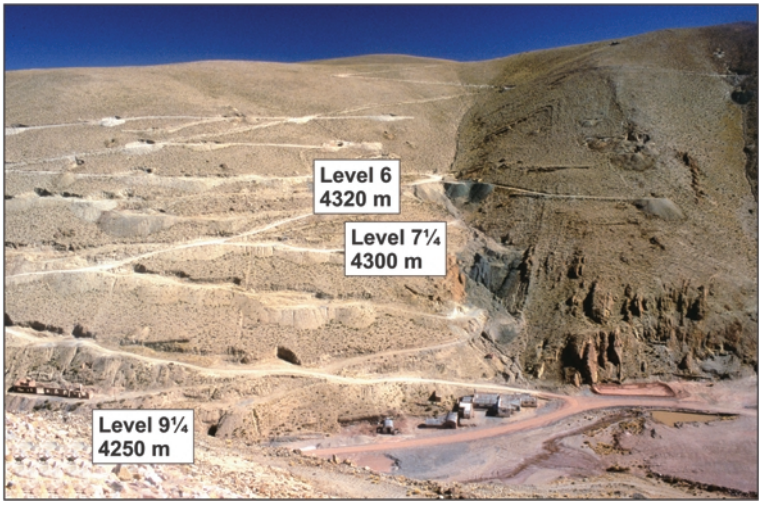

FIG. 2. Photograph from N of the Oploca vein system with major levels. The anticlinal structure is clearly visible in the more shadowy part of the slope, just to the right of the major (greenish-grey) dumps. The new ramp to the downward continuation of the Oploca vein system was constructed at the valley floor and the entrance is just visible at the right edge of the photo.

crustification, symmetrical banding, vugs and comb, cockade and colloform structures (Figs 3–5). The boundary with the host silicified metapelites is very sharp. A stockwork of crosscutting veinlets and mineralized fissures, however, is frequently present in the hanging wall and footwall of major veins. Pinch-and-swell structures are very common. Ore shoots of variable size containing high-grade Ag-Sn mineralization alternate with low-grade sections where pyrite-marcasite-sphalerite may be the only sulphides present in the veins.

Mineralogy of veins

Based on the mineral assemblages within the veins, four different vein types can be distinguished at Oploca (Paar *et al.*, 2006*b*). However, these types represent end-members, and gradations between the various types may occur.

Type 'A' veins are characterized by a sequence of alternating bands of sphalerite–wurtzite, suredaite, coiraite, franckeite, and minor amounts of irregularly distributed grains of members of the rhodostannite–toyohaite and hocartite–pirquitasite solid solution series (Paar *et al*., 1998, 2000, 2001). Typical examples are exposures of the northern Oploca vein ('Veta Oploca Norte') at the level 9¼ (Fig. 3*a,b*) and most, if not all, exposures at the sublevels 1–6 accessible between the main levels 7¼ and 6 (Fig. 4).

Type **'B'** veins are represented by an especially high-grade Ag-Sn mineralization, which is dominated by intermediate members of the hocartite–pirquitasite solid-solution series and pyrite-marcasite. The only vein bearing this type of mineralization occurred at the Oploca crosscut; it was named the southern vein ('Veta Oploca Sur') and was recently mined out.

Type 'C' veins are also typified by high-grade Ag mineralization, but with a completely different mineral assemblage, which comprises Ag-Sb sulphosalts (andorite IV, fizelyite, miargyrite,

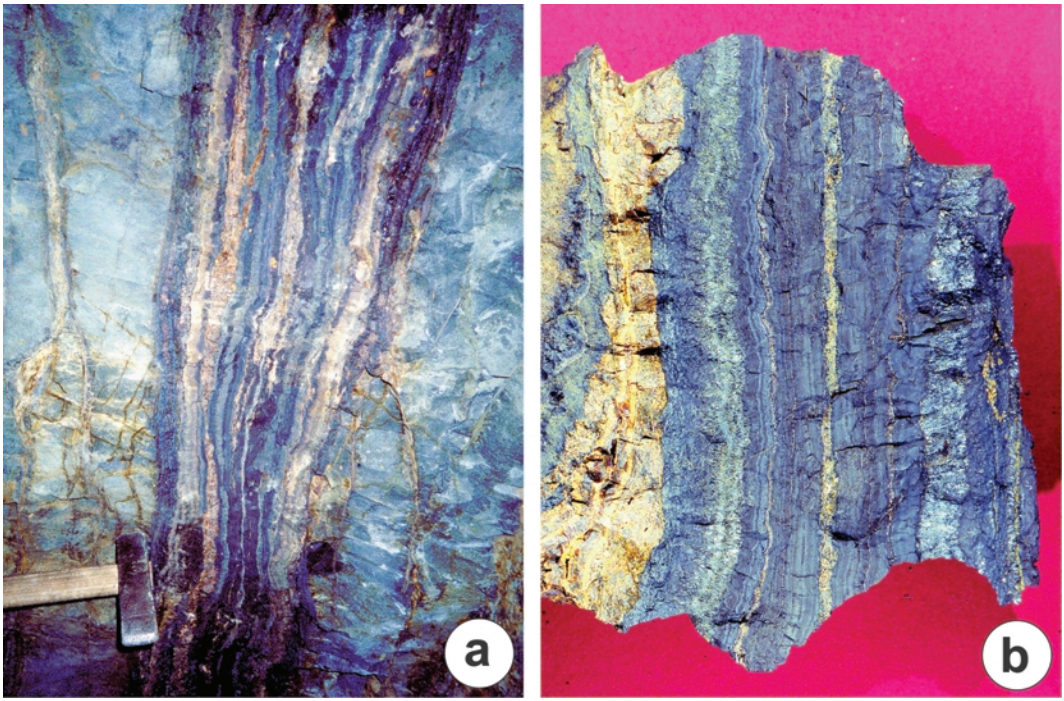

FIG. 3. (*a*) The northern vein ('Veta Norte') at the main level 9¼ as it was exposed around the year 2000. It is ~315 m from the entrance of the crosscut. This vein is an excellent example of symmetrical banding, and is composed of alternating bands of coiraite, suredaite and sphalerite–wurtzite. The width of the banded vein is ~0.4 m. (*b*) Detail of (*a*) showing the assemblage coiraite (laminated, fine-grained), two layers of suredaite in approximately the same distance to the right and left of the central veinlet of yellowish-coloured sphalerite. Width of sample: 10 cm.

FIG. 4. Exposed banded-vein section (thickness 0.3 m) of two parts: to the left, a symmetrical vein can be seen, with sphalerite (centre) and suredaite flanking it; to the right, a later stage of mineralization occurs with colloform-textured laminated bands of coiraite as the dominant constituent and a centre-line veinlet of suredaite. Oploca, level 7¼.

FIG. 5. Large fragments of broken and highly silicified metapelites of the Acoite Formation are rimmed by thick seams of crystallized suredaite which forms large druses and fills interstices in the country rock. Oploca, level 7¼. Length of the large cavity ~0.2 m.

traces of pyrargyrite), cylindrite, franckeite and reniform sphalerite. A typical vein is exposed at level 8, sublevel 5.

Type 'D' veins are characterized by a combination of the mineral assemblages of type 'A' and 'B' veins; they represent the most economically important vein types and have been mined extensively between the levels 8 and 9¼. Some of the remaining ore is still exposed at level 8 (sublevel 4).

Type 'A' veins exposed at the sublevels (1–6) of level 7¼ are enriched in coiraite and suredaite, associated with minor franckeite, sphalerite and pyrite-marcasite. Local ore shoots are almost monomineralic with suredaite as the dominant sulphide. The most spectacular mineralization of this type is exposed at sublevel 4 where vein sections with massive suredaite, as aggregates of intergrown needles, are frequently accompanied by vugs and cavities up to 20 cm in length lined with beautiful crystals of this mineral (Figs 5–7). Of particular note are exposures within tectonized and altered country rocks where individual rock fragments are surrounded by thick crusts and crystals of suredaite.

The thickness of all vein types is quite variable and may range from a few centimetres to >>1 m. Almost certainly, veins with much greater thicknesses have been mined in the past, as is clearly reflected by huge mined-out stopes in the Oploca system between levels 7¼ and 9¼.

The vein system at Oploca cuts across a large breccia body which is very well exposed at sublevels 1–4 of level 7¼ (Fig. 5). This breccia is composed of extremely silicified fragments of the country rock, which may also show argillic alteration (formation of kaolinite). Both a Ag- and a Sn-enriched breccia may be observed in the vicinity of the major veins (type 'A') (Paar *et al.*, 2006 *a*,*b*).

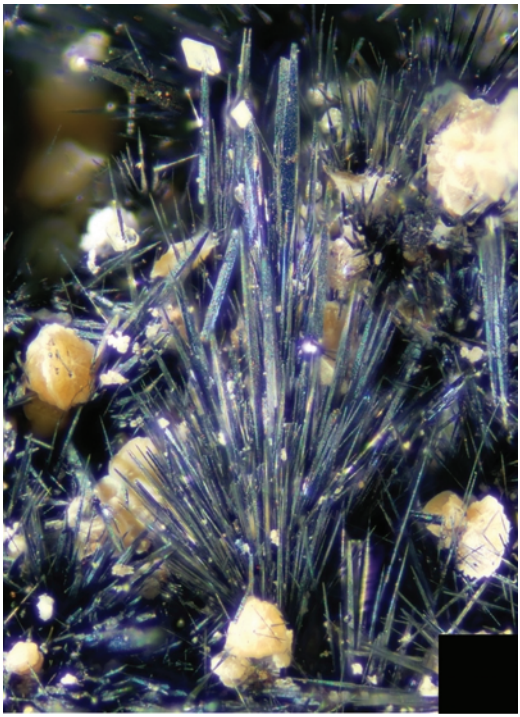

FIG. 6. Spear-shaped crystals of suredaite in radial sprays protruding from the country rock. The crystals attain a length of >1 cm and are frequently associated with balls of siderite. Oploca, level 7¼. Length of crystal sprays attains 1 cm.

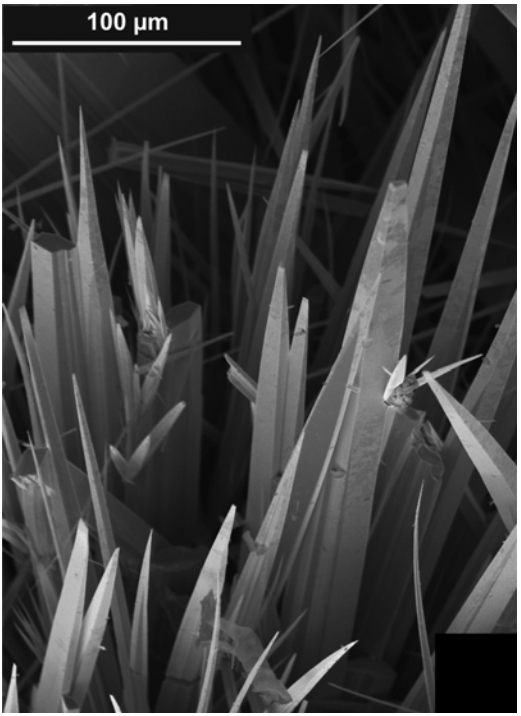

FIG. 7. SEM image of suredaite crystals (courtesy of Dr Ronald Miletich). Oploca, level 7¼.

The abundance of both coiraite and suredaite clearly indicates their significant contribution to the grade of Sn in the ore, and thus their economic importance. However, their occurrence is more or less limited to the uppermost 100–120 m of the Oploca vein system. Both minerals subsequently disappear below the level 9¼.

Coiraite: appearance and physical properties

Layers of coiraite, which attain a thickness of several centimetres, are composed of very dense, earthy and fine-grained aggregates with a distinct colloform texture (Figs 3*b*, 4) and resemble oxidized manganese ore. The associated minerals are minor pyrite and marcasite, galena, micrometre-sized cassiterite and arsenopyrite, as well as traces of intermediate members of the hocartite–pirquitasite and rhodostannite–toyohaite series.

Microscopically, laminae of coiraite consist of extremely thin bent platy crystals which are deformed (Fig. 8*a*,*b*). Arborescent and reticulated forms are common. Individual crystals typically range between a few µm and 10 µm in length, but rare lamellae up to 50 µm long were observed.

In hand specimen, coiraite is grey to dark-grey with a dark-grey to almost black streak. The natural material is dull. Mohs hardness is impossible to determine, but is probably <2. Synthetic material was produced to determine the physical properties on coarser crystallized material (compare the section on 'Coiraite synthesis'). The product shows flakes up to 1 mm long, which are flexible, inelastic, slightly malleable, and have a perfect cleavage parallel to a basal plane. Their lustre is metallic, very similar to franckeite. VHN_{10} has a range between 61 and 93 (average 74) kg/mm^2, corresponding to a Mohs hardness close to 2.

The density of the natural mineral could not be measured because of the pervasively intergrown occurrence. Using the general formula $Me_{3.607}S_{4.685}$ (*Me*: metals and other cations) and $Z = 2$, the calculated density is 5.92 g/cm^3, slightly lower than that of franckeite, 6.02 g/cm^3

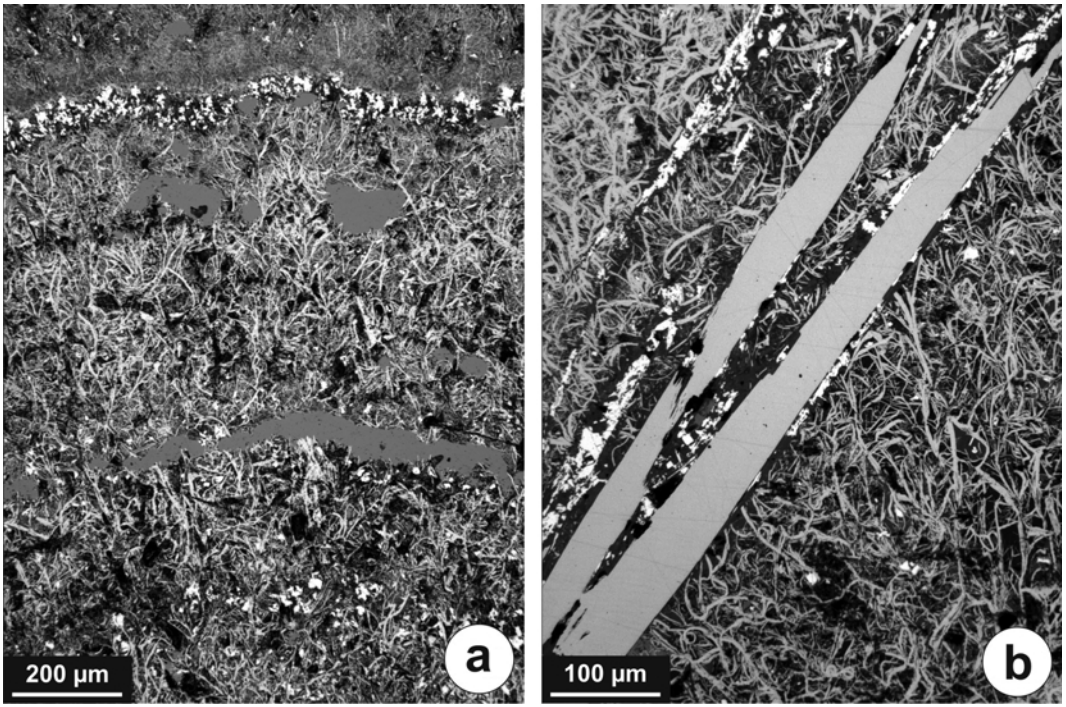

FIG. 8. (*a*) Bands of microcrystalline coiraite, showing arborescent and reticulated forms, alternating with sphalerite (grey, homogeneous) and a single band containing disseminations of galena. Oploca, level 9¼. (*b*) Coiraite (in arborescent forms) with embedded crystals of suredaite which are seamed by galena (white). Oploca, 7¼. Polished sections PI/COI 23,24; air, 1 polar.

(Mottana *et al*., 1992). The density of the synthetic and slightly porous product was determined using a Berman microbalance on two fragments weighing 25.1 and 31.4 mg, respectively. Their densities are 5.85 and 5.87, respectively, thus very close to the calculated density.

Optical properties

In polished section in plane polarized light (~3200 K), coiraite has a bluish-grey colour against galena, and does not show any discernible pleochroism. The bireflectance is very weak in air and oil. Coiraite is moderately anisotropic in oil and the rotation tints are brown to bluish-grey.

Reflectance data for coiraite were obtained in air from 400–700 nm using a Zeiss Axiotron microscope equipped with a Crystal Structures (Lanham) specimen – standard levelling super-stage and a J & M Tidas diode-array spectrometer. Measurements were made relative to a Zeiss WTiC standard using Cavendish Instruments Onyx software at intervals of 0.823 from 400–700 nm.

The results are summarized in Table 1 and Fig. 9. In terms of reflectance and overall optical properties, there is very little difference between coiraite and the closely related sulphosalt franckeite. In comparison with the latter, it can be seen that R_1 and R_2 of franckeite (using the values of Caye and Pasdeloup, 1975, quoted in QDF3 of Criddle and Stanley, 1993) roughly bracket the data for the apparently less-bireflectant coiraite. This difference, however, may not be real, and could be related to the orientation of those crystals which were suitable for the measurement.

Chemical composition

Most of the polished sections contain coiraite in a grain size which is too small to permit reliable quantitative analysis. Considerable efforts were expended to locate lamellae suitable for analyses and special techniques were applied to produce high-quality polished sections.

TABLE 1. Reflectance data and colour values for coiraite (Pirquitas) compared to franckeite (Poopó, Bolivia).

	Coiraite (Pirquitas)		Franckeite (data of Caye and Pasdeloup, QDF 3.175 in Criddle and Stanley, 1993)	
λ (nm)	R_1%	R_2%	R_1%	R_2%
400	38.9	39.9	38.2	39.4
420	38.3	38.9	37.9	39.2
440	37.7	38.3	37.6	39.0
460	37.3	38.0	37.3	38.7
480	36.9	37.8	36.9	38.5
500	36.6	37.6	36.6	38.2
520	36.3	37.4	36.2	37.9
540	36.0	37.2	35.8	37.6
560	35.7	36.8	35.4	37.3
580	35.3	36.5	35.0	36.9
600	35.0	36.0	34.6	36.5
620	34.6	35.7	34.2	36.1
640	34.1	35.1	33.8	35.7
660	33.6	34.7	33.4	35.3
680	33.1	34.1	33.0	34.9
700	32.6	33.6	32.6	34.5
	COM[1]			
470	37.1	37.9	37.15	38.6
546	35.9	37.1	35.65	37.65
589	35.15	36.3	34.85	36.7
650	33.9	34.9	33.6	35.5
	Colour values			
C illuminant				
x	0.304	0.305	x 0.303	0.304
y	0.312	0.313	y 0.311	0.312
Y%	35.7	36.8	Y% 35.5	37.3
λ_d	481	484	λ_d 481	482
Pe (%)[2]	2.8	2.3	Pe% 3.3	2.6

[1] Commission on Ore Mineralogy of the International Mineralogical Association
[2] Excitation purity

Chemical analysis was done at the Department of Materials Engineering and Physics (Division of Mineralogy), University of Salzburg, using a JEOL Superprobe JXA-8600, in wavelength dispersive spectrometry mode, controlled by a LINK−*exL* system, operated at 25 kV and 25 nA, and a beam diameter of 4 μm. The following standards and emission lines were used: galena (Pb-*M*α), nickeline (As-*L*α), pyrite (Fe-*K*α) and stibnite (Sb-*L*α, S-*K*α), and Ag (Ag-*L*α) and Sn (Sn-*L*α) metals. The raw data were corrected with the on-line ZAF-4 procedure. The analytical results are presented in Table 2.

Individual crystals (flakes) are chemically homogeneous and there is only slight variation between lamellae in the same section. The analytical results of 36 spot analyses using material from different locations between the crosscut at the level 9¼ (4250 m above sea level) and the sublevels above the level 7¼ (4300 m above sea level) show the following range of element composition (wt.%): Pb 50.91−55.43, Sn 16.83−20.05, Fe 1.27−1.81, Ag 0−0.41, As 4.75−5.84 and S 20.57−22.34. The average composition using the data (31 point analyses) from level 9¼, where coiraite is the most abundant, is (wt.%): Pb 54.68, Sn 17.13, Fe 1.45, Ag 0.33, As 5.27 and S 21.14, total 100.00, leading to the empirical formula (with S = 28 atoms): $Pb_{11.21}As_{2.99}Ag_{0.13}Fe_{1.10}Sn_{6.13}S_{28.00}$. This is very close to the ideal formula $(Pb_{11.3}Sn^{2+}_{1.2})_{\Sigma=12.5}Fe^{2+}Sn^{4+}_5As_3S_{28}$, which requires

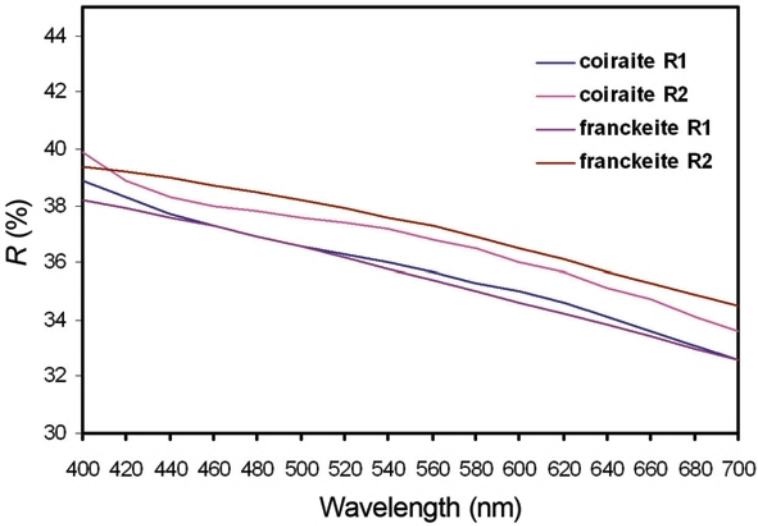

FIG. 9. Reflectance spectra in air for coiraite and franckeite.

Pb 59.38, As 5.15, Sn 13.61, Fe 1.28, S 20.58, total 100.00.

Electron diffraction and X-ray crystallography

Electron diffraction data for small fragments extracted from the sample were studied using a JEM-100C microscope. Selected area electron diffraction (SAED) patterns from fragments with different inclinations to the electron beam were obtained. The type of SAED pattern for coiraite with strong *Q* (pseudotetragonal) and *H* (pseudohexagonal) subcell reflections is shown in Fig. 10. The pattern displays different distributions of intensities; stronger reflections corresponding to the *Q* subcell and weaker reflections to the *H*

TABLE 2. Chemical composition (wt.%) of coiraite from Pirquitas, Argentina.

Location	*n*[1]		Pb	As	Ag	Fe	Sn	S	Total
Oploca 9¼	31	mean	54.68	5.27	0.33	1.45	17.13	21.14	100.00
Level 0		s.d.[2]	0.43	0.41	0.16	0.17	0.25	0.29	0.59
Veta Norte									
Oploca 7¼	5	mean	51.55	5.32	0.00	1.61	19.90	22.06	100.44
Sublevel +6		s.d.[2]	0.43	0.06	0.00	0.04	0.08	0.29	0.75
Veta 4									
Synthesis	18	mean	53.39	4.20	0.15	1.74	18.84	21.24	99.55
		s.d.[2]	0.48	0.23	0.06	0.05	0.56	0.16	0.41

	Formula (S = 28)						
	Pb	As	Ag	Fe	Sn	S	Σ*Me*
Oploca 9¼	11.21	2.99	0.13	1.10	6.13	28.00	21.56
Oploca 7¼	10.13	2.89	0.00	1.17	6.82	28.00	21.01
Synthesis	10.89	2.37	0.06	1.31	6.71	28.00	21.34

[1] number of spot analyses
[2] standard deviation

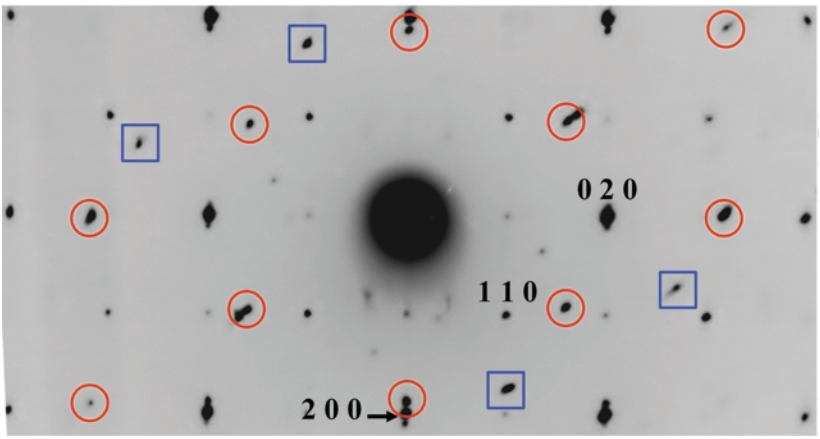

FIG. 10. *hk*0 electron diffraction pattern of coiraite. Indexed reflections refer to the *Q*-subcell. Reflections of the *H*-subcell are shown by red circles; strong reflections fitting neither the *H*- nor the *Q*-subcell are indicated by blue squares.

subcell, which may be dependent on differences in the composition of layers. This SAED pattern gave $a_0 \approx b_0 \approx 5.91$ Å for the *Q* subcell and $a_0 \approx 6.33$ Å and $b_0 \approx 3.67$ Å for the *H* subcell. The ratio of the areas of the *Q* and *H* sub-cells represented by coefficient $k = S_Q / 2S_H$ (Organova, 1989) is 0.752. The relation between a_0 for both *Q* and *H* subcells is ~13 $a_Q \approx 12\ a_H$ These characteristics correspond to a franckeite-like structure (Makovicky and Hyde, 1992).

X-ray powder-diffraction data for the same samples were obtained using a 114.6 mm Debye-Scherrer camera and also a powder diffractometer corrected with Si as an internal standard (Table 3). The sub-cell parameters were refined by least-squares from the X-ray powder diffraction data using the approximate values from electron diffraction studies and published data for franckeite and potosiite (computer programs *SPECTR*) with monoclinic symmetry (space group *P*2/*m*). The X-ray data were indexed using the program *RD-230* for the *Q* and *H* subcells based on monoclinic symmetry. The choice criterion for the *H* subcell indices became at this point *Am* (according to Mottana *et al*., 1992; Wolf *et al*., 1981; Shimizu *et al*., 1992). The final unit-cell refinement was done after this operation (see Table 3).

A comparison of two diffraction patterns shown in Table 3 indicates that the first diffraction line is missing. This is the result of a higher starting angle in the diffractometer experiment ($d = 8.63$ Å, (*hkl*) = (002) for the *Q*-subcell, and $d = 8.62$ Å with the same indices for the *H*-subcell). Some unindexed lines are due to unidentified impurities. The unit cells are very similar for both X-ray patterns. There are some differences in the intensities of certain reflections, mainly due to preferred orientation by the diffractometer method.

Crystal chemistry

Relation to other layered chalcogenides

Coiraite belongs to the cylindrite group of complex Pb sulphosalts with incommensurate composite-layered structure (Makovicky and Hyde, 1992; Moëlo *et al*., 2008). There are also many synthetic chalcogenides of this type (Wiegers and Meerschaut, 1992). All these structures result from the regular stacking of two kinds of layers: in cylindrite, one layer corresponds to a $(100)_{PbS}$ slab which is two-atoms-thick (pseudotetragonal *Q* layer), and the other layer to a single SnS_2-type octahedral layer (pseudohexagonal *H* layer). Defining the common stacking periodicity as *c*, the in-plane parameters a_Q and b_Q, and a_H and b_H, are generally parallel, but the ratios a_Q/a_H and b_Q/b_H are irrational. Franckeite is a higher homologue of cylindrite, with a four-atom-thick *Q* layer (Williams and Hyde, 1988), and coiraite is thus the homeotypic As-derivative of franckeite.

Cylindrite and franckeite are complex sulphosalts of Pb, Sn, Sb and Fe. According to Makovicky (1974), the *Q* layer of cylindrite, with general formula *Me*S, contains all the Pb

TABLE 3. X-ray powder-diffraction data for coiraite.

X-ray powder-diffraction data for coiraite (camera)*						X-ray powder-diffraction data for coiraite (diffractometer)					
Coiraite (obs.)		*Q*-subcell (calc.)		*H*-subcell (calc.)		Coiraite (obs.)		*Q*-subcell (calc.)		*H*-subcell (calc.)	
I/I_0	*d*	*d*	*hkl*	*d*	*hkl*	I/I_0	*d*	*d*	*hkl*	*d*	*hkl*
10	8.55	8.63	002	8.62	002						
20	5.78	5.76	003	5.74	003	19	5.83	5.76	003	5.78	003
40	4.34	4.32	004			61	4.27	4.32	004		
20	4.12										
10	3.814	3.801	$11\bar{2}$			47	3.814	3.803	$11\bar{2}$		
5	3.615	3.586	$10\bar{4}$								
30br	3.460	3.454	005	3.446	005	72	3.426	3.456	005	3.469	005
20	3.339	3.361	104			87	3.345	3.358	104		
10	3.215					42	3.219				
15br	3.132			3.127	$11\bar{1}$	78	3.122			3.117	$11\bar{1}$
5	3.003			2.994	$20\bar{2}$	71	3.009			2.974	$20\bar{2}$
15	2.959	2.977	015	2.957	112	94	2.966	2.977	015	2.958	112
100br	2.876	2.878	006	2.872	006	100	2.883	2.880	006	2.890	006
5	2.767	2.781	022	2.797	$11\bar{3}$	30	2.767	2.776	022	2.788	$11\bar{3}$
10	2.700	2.704	202	2.721	202	25	2.702	2.702	202		
15	2.640	2.652	$10\bar{6}$			33	2.646	2.658	$10\bar{6}$		
3	2.618	2.616	023								
5	2.483	2.488	122	2.500	204						
5br	2.414	2.414	$12\bar{3}$			11	2.406	2.413	$12\bar{3}$		
3	2.359	2.359	123			12	2.375	2.355	123		
5	2.273	2.272	$12\bar{4}$			14	2.278	2.271	$12\bar{4}$		
5	2.231	2.237	025								
10	2.163	2.165	$11\bar{7}$	2.162	$20\bar{6}$	13	2.164	2.168	$11\bar{7}$	2.153	$20\bar{6}$
3	2.129	2.120	$12\bar{5}$								
5	2.098			2.085	206	40	2.097			2.100	206
60	2.068	2.068	220			51	2.065	2.066	220		
10	2.023	2.023	215			31	2.028	2.021	215		
3	1.988	1.989	222			11	1.975	1.987	222		
5	1.965	1.968	$12\bar{6}$	1.962	$11\bar{7}$					1.962	$11\bar{7}$
5	1.934	1.941	300								
5	1.908	1.910	032	1.906	207	36	1.915	1.906	032	1.922	207
15	1.830	1.901	$22\bar{4}$	1.833	020	23	1.823			1.830	020
15	1.812	1.813	$22\bar{5}$					1.814	$22\bar{5}$		
10	1.787	1.787	109	1.793	022	42	1.788	1.786	109	1.790	022
10	1.763	1.770	127			33	1.764	1.768	127		
						16	1.749	1.752	133		
						18	1.709	1.709	119		
						9	1.674	1.679	208		
						16	1.633				
						2	1.552	1.553	209	1.552	222
						8	1.495	1.498	$12\bar{7}$		
						5	1.483			1.480	$31\bar{7}$
						7	1.439	1.438	$23\bar{6}$		
		a = 5.86(1) Å b = 5.86(1) Å c = 17.37(1) Å α = 90.0° β = 94.55(1)° γ = 90.0° V = 596(1) Å^3		a = 6.28(1) Å b = 3.66(1) Å c = 17.31(1) Å α = 90.0° β = 92.25(3)° γ = 90.0° V = 397(3) Å^3				a = 5.84(1) Å b = 5.86(1) Å c = 17.32(1) Å α = 90.0° β = 94.14(1)° γ = 90.0° V = 590(1) Å Z = 4 0.997:1:2.955		a = 6.28(1) Å b = 3.66(1) Å c = 17.33(1) Å α = 90.0° β = 91.46(1)° γ = 90.0° V = 398(1) Å Z = 2 1.716:1:4.735	

* 114.6 mm Debye-Scherrer powder camera; Cu radiation, Ni-filter (λ Cu-$K\alpha$ = 1.54178 Å). Intensities visually estimated. Not corrected for shrinkage, and no internal standard.

TABLE 4. In-plane parameters and related unit surface for layered chalcogenides with a four-atom-thick $(100)_{PbS}$ slab.

	In-plane parameters (Å)		In-plane angle (°)	In-plane unit surface (Å^2)
	lowest	highest		
Nagyágite[(1)]	5.937*	5.937*	89.40	35.25
Franckeite ('Potosiite')[(2)]	5.84	5.88	90	34.34
Coiraite[(3)]	5.839	5.862	90	34.23
'Franckeite-Nb'[(4)]	5.8285	5.864	89.97	34.18
Lengenbachite[(5)]	5.842	5.847	91.01	34.16
Franckeite ('Incaïte')[(6)]	5.79	5.83	90	33.76
$Ca_2Sb_2S_5$[(7)]	5.689**	5.694**		32.39

* centred supercell; ** sub-cell
[(1)] Effenberger *et al.* (1999); [(2)] Wolf *et al.* (1981); [(3)] This study; [(4)] Lafond *et al.* (1997); [(5)] Makovicky and Hyde (1992); [(6)] Makovicky (1974); [(7)] Cordier and Schäfer (1981).

atoms, together with Sn^{2+} and the main part of Sb, while the *H* layer, with formula *Me*'S_2, contains major Sn^{4+} and Fe^{2+}. The detailed crystal structure of cylindrite is not known at present, but that of a synthetic Sn-Se derivative was solved recently (Makovicky *et al.*, 2008). In synthetic lévyclaudite-(Sb), the Cu derivative of cylindrite, the *Q* layer contains Pb and Sb only, while the *H* layer contains Sn^{4+} and Cu (Evain *et al.*, 2006).

The precise crystal structure of franckeite is also not known, but the cation partitioning between the two constituent layers is similar to that in cylindrite, with Pb, Sn^{2+} and Sb in the *Q* layer, and Sn^{4+} and Fe in the *H* layer. The chemical nature of the *Q* layer is confirmed by the crystal structure of synthetic 'franckeite-Nb' (Lafond *et al*., 1997), where a franckeite-type *Q* layer alternates with a NbS_2 layer of the MoS_2 type. Here, the *Q* layer contains Pb and Sb as cations, with Sb concentrated exclusively in the two inner slabs (40 at.%).

Similarly, it is assumed that in coiraite, the *Q* layer probably contains Pb, Sn^{2+} and As, and the *H* layer only Sn^{4+} and Fe. There are other known structures with the same type of *Q* layer found in franckeite and coiraite: lengenbachite (Williams and Pring, 1988), 'franckeite-Nb' (Lafond *et al*., 1997), nagyágite (Effenberger *et al*., 1999) and synthetic $Ca_2Sb_2S_5$ (Cordier and Schäfer, 1981). Table 4 compares the in-plane parameters and in-plane surfaces of these compounds. 'Potosiite' (Wolf *et al*., 1981) corresponds to pure Sn^{2+}-free franckeite, while 'incaite' is a Sn^{2+}-rich franckeite (Makovicky, 1974). It seems that the in-plane size of the *Q* layer decreases according to: (1) the size of the divalent cation [Pb^{2+} ('potosiite') → Sn^{2+} ('incaite') → Ca^{2+} ($Ca_2Sb_2S_5$)], (2) the size of the trivalent cation [Sb^{3+} (franckeite) → As^{3+} (coiraite)] and (3) the fraction of the trivalent cation substituting for the divalent cation. This last substitution may explain why, in the *Q* layer of coiraite, an As-member has a larger size in-plane surface than does 'franckeite-Nb', an Sb member.

Crystal chemical formula of coiraite

According to the available data, the *Q* and *H* unit subcell surfaces of coiraite are respectively:

$$S_Q = a_Q \times b_Q = 5.839 \times 5.862 = 34.228 \text{ Å}^2$$
$$S_H = a_H \times b_H = 6.278 \times 3.660 = 22.977 \text{ Å}^2$$

As the two *Q* and *H* subcells correspond to centred pseudotetragonal and pseudohexagonal (orthogonal setting) lattices, they contain $[4(Me_2S_2)]$ and $[1(Me'_2S_4)]$ atoms, respectively. For the whole structure, considering one unit *H* subcell, which contains $[1(Me'_2S_4)]$ atoms, for the same volume, the *Q* part will correspond to $([4(Me_2S_2)] \times S_H/S_Q)$ atoms. As $S_H/S_Q = 0.6713$, the structural formula can be written as:

$$[4(Me_2S_2)]_{0.671} \cdot [1(Me'_2S_4)] \text{ or } (Me_4S_4)_{0.671} \cdot (Me'S_2) \quad (1)$$

Formula 1 gives a total of 3.69 metal atoms, and 4.69 S atoms (ratio metal/S = 0.787). According to the electron microprobe results, the mean composition, on the basis of $\Sigma_{cations}$ = 3.69 atoms is:

$$(Pb_{1.92}As_{0.51}Fe_{0.19}Ag_{0.02}Sn_{1.05})_{\Sigma=3.69}S_{4.79} \quad (2)$$

There is a slight excess of S atoms (~2%), which is within analytical error. If there is only Sn and Fe in the *H* layer, according to formula (2) the total (Sn + Fe) exceeds 1 atom (= 1.24 atoms), indicating that a fraction of the Sn (the excess relative to 1, i.e. 0.24 atoms, corresponding to 23 at.% of total Sn) is in the divalent state, substituting for Pb in the *Q* layer. In the mean microprobe analysis (Table 2), the relative error on the charge balance (Ev) with Sn^{4+} exclusively is +12.2%; with 23 at.% Sn as Sn^{2+}, the corrected Ev value is −0.8%, which fits neutrality. The formula (without S excess) then becomes:

$$[(Pb_{1.92}Sn^{2+}_{0.24}As_{0.51}Ag_{0.02})_{\Sigma=2.69}S_{2.685}]^{0.49+} [(Sn^{4+}_{0.81}Fe_{0.19})_{\Sigma=1}S_2]^{0.39-} \quad (3)$$

or, to adjust it as in formula 1:

$$[(Pb_{2.85}Sn_{0.35}As_{0.76}Ag_{0.03})_{\Sigma=4}S_4]_{0.67}\cdot [(Sn_{0.81}Fe_{0.19})_{\Sigma=1}S_2] \quad (4)$$

In formula 3, it can be seen that there is a slight excess of positive charge (+0.10) of the *Q* layer relative to the negative charge in the *H* layer. Normally, the positive charge of the *Q* layer, due to the As^{3+} (minus Ag), is twice the Fe^{2+} content of the *H* layer, according to the heterovalent substitution $2\ Pb^{2+} + Sn^{4+} \rightarrow 2\ As^{3+} + Fe^{2+}$. Here one has the ratio (As−Ag)/Fe = 2.58, which may indicate a more complex crystal chemistry, e.g. some As in the *H* layer (see section on examination of EPM analyses below).

Stoichiometric approximation

In coraite, the ratio $b_Q/b_H = 1.602$ is very close to 8/5, corresponding to a good quasi-commensurate approximation: $8\ b_H \sim 5\ b_Q$. However, the ratio $a_Q/a_H = 0.9301$ does not fit with the ratio of two small integers (it is between 13/14 = 0.929, and 14/15 = 0.933). Consequently, it is not possible to propose a stoichiometric formula. Nevertheless, a simplified formula can be proposed if one considers that the ratio S_H/S_Q (= 0.671) is close to 2/3 (relative error of 0.7%). In formula 3, multiplying all coefficients by 3 gives:

$$[(Pb_{5.75}Sn_{0.71}As_{1.53}Ag_{0.07})_{\Sigma=8.06}S_{8.06}]\cdot [(Sn_{2.43}Fe_{0.57})_{\Sigma=3}S_6]$$

with $2\ Pb^{2+} \rightarrow As^{3+} + Ag^{+}$:

$$[(Pb_{5.88}Sn_{0.71})_{\Sigma=6.59}As_{1.46}S_{8.06}]\cdot[(Sn_{2.43}Fe_{0.57})S_6]$$

multiplied by 2:

$$[(Pb_{11.76}Sn_{1.42})_{\Sigma=13.18}As_{2.93})S_{16.11}]\cdot [(Sn_{4.87}Fe_{1.13})S_{12}]$$

leads to the simplified formula

$$[(Pb_{0.9}Sn_{0.1})_{14}As_2S_{16}]^{2+}\cdot[Sn_5FeS_{12}]^{2-}$$

Detailed examination of EPM analyses of coiraite and associated franckeite and cylindrite

Thirty-six spot analyses of coraite were collected. Table 5*a* gives the final set of spot or mean analyses, including two analyses of franckeite and two of cylindrite. Analysis P117-d, corresponding to cylindrite, is clearly distinguished by its lower *Me*/S atomic ratio (~0.68, against 0.74−0.78 for coiraite and franckeite – see Makovicky and Hyde, 1991). Table 5*b* gives the structural formulae based on 3.69 *Me* atoms, according to the incommensurate ratio between the *Q* and *H* layers. With Sn exclusively as Sn^{2+}, the charge is always negative; therefore charge-balance was obtained by adjusting the Sn^{4+}/Sn^{2+} ratio. Figure 11 shows a positive correlation between these two cations; such a correlation is controlled by the charge transfer between *Q* and *H* layers. As a general rule for 2D-misfit compounds (Meerschaut *et al*., 2000), one Fe^{2+} atom substituting for a Sn^{4+} atom in the *H* layer is equilibrated by two As^{3+}

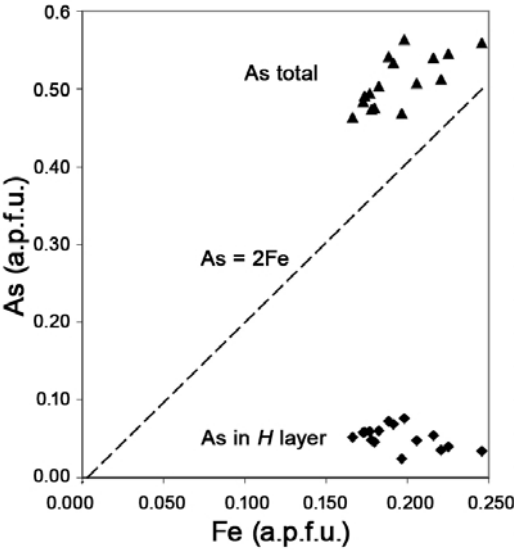

FIG. 11. Correlation between As and Fe (a.p.f.u.), considering the As total, and the As fraction within the *H* layer.

TABLE 5*a*. Electron microprobe analyses of coiraite and associated franckeite/cylindrite: (wt.% elements).

Sample	n[1]	Pb	As	Sb	Sn	Fe	Ag	S	Sum
Oploca 7¼,6,4 A	5	51.55	5.33	0.00	19.90	1.61	0.00	22.06	100.45
Oploca 7¼,6,4 B	1	51.13	5.74	0.00	17.52	1.88	0.00	21.82	98.09
Oploca 02/86 A	1	53.29	5.47	0.00	16.46	1.63	0.00	21.35	98.20
Oploca 02/86 B	3	53.36	5.23	0.00	17.17	1.68	0.00	21.37	98.81
Pir-2 A	2	54.10	4.90	0.00	18.10	1.50	0.40	21.30	100.22
Pir-2 B	2	54.65	5.75	0.00	17.10	1.77	0.24	21.50	101.01
PI/3 A	4	54.85	5.03	0.00	17.13	1.33	0.39	20.95	99.66
PI/3 B	2	54.95	4.75	0.00	17.70	1.27	0.41	21.20	100.28
PI/3 C	3	54.37	5.63	0.00	17.20	1.46	0.31	21.37	100.33
PI/3 D	1	54.90	4.90	0.00	17.60	1.38	0.37	21.10	100.25
PI/3 E	1	53.80	5.80	0.00	16.60	1.52	0.22	21.10	99.04
PI/3 F	1	54.30	5.50	0.00	17.00	1.47	0.20	21.20	99.67
PI 98/3 A	3	54.43	5.07	0.04	17.30	1.35	0.37	21.07	99.63
PI 98/3 B	2	54.70	5.15	0.06	16.80	1.39	0.33	21.10	99.53
PI 98/3 C	2	54.00	4.80	0.04	17.35	1.35	0.35	21.15	99.04
PI 98/3 D	3	54.43	4.93	0.08	17.27	1.31	0.40	21.23	99.66
mean		53.92	5.25	0.01	17.39	1.49	0.25	21.30	99.62
s.d.[2]		1.13	0.36	0.03	0.78	0.18	0.16	0.29	0.82
PI17-h Franckeite	2	52.90	0.18	10.00	13.40	1.58	1.20	20.60	99.86
PI17-d Cylindrite	2	41.70	0.56	11.00	19.95	1.78	0.60	23.85	99.43

[1] number of analyses
[2] standard deviation

TABLE 5*b*. Structural formulae on the basis of a total of *Me* = 3.685 atoms (2.843 atoms for cylindrite). The As/Fe values are in fact (As–Ag)/Fe for coiraite and (Sb–Ag)/Fe for franckeite and cylindrite.

Sample	Pb	As	Sb	Sn	Fe	Ag	S	ΣVal1	Sn^{4+}	Sn^{2+}	Sn^{2+}/Sn^{4+}	As/Fe	*Me*/S	*Me*(Q)	As(Q)	Sn^{4+}+Fe	As(H)	CT[2]
Oploca 7¼,6,4 A	1.775	0.507	0.00	1.196	0.206	0.00	4.910	−1.9	0.747	0.450	0.60	2.46	0.751	2.733	0.460	0.952	0.048	0.60
Oploca 7¼,6,4 B	1.802	0.559	0.00	1.078	0.246	0.00	4.969	−2.0	0.720	0.358	0.50	2.28	0.742	2.719	0.526	0.966	0.034	0.63
Oploca 02/86 A	1.903	0.540	0.00	1.026	0.216	0.00	4.927	−1.9	0.730	0.296	0.41	2.50	0.748	2.739	0.486	0.946	0.054	0.65
Oploca 02/86 B	1.890	0.513	0.00	1.062	0.221	0.00	4.891	−1.9	0.744	0.318	0.43	2.32	0.754	2.721	0.477	0.964	0.036	0.58
Pir-2 A	1.889	0.469	0.00	1.104	0.196	0.027	4.810	−1.8	0.779	0.325	0.42	2.25	0.766	2.710	0.444	0.975	0.025	0.49
Pir-2 B	1.875	0.545	0.00	1.024	0.225	0.016	4.766	−1.6	0.735	0.289	0.39	2.35	0.773	2.725	0.506	0.960	0.040	0.61
PI/3 A	1.938	0.491	0.00	1.056	0.174	0.026	4.783	−1.7	0.768	0.289	0.38	2.68	0.770	2.744	0.432	0.941	0.059	0.58
PI/3 B	1.938	0.463	0.00	1.090	0.166	0.027	4.832	−1.9	0.782	0.308	0.39	2.62	0.763	2.737	0.412	0.948	0.052	0.54
PI/3 C	1.891	0.542	0.00	1.044	0.188	0.020	4.801	−1.7	0.739	0.305	0.41	2.77	0.768	2.757	0.469	0.928	0.072	0.67
PI/3	1.927	0.476	0.00	1.078	0.180	0.025	4.785	−1.7	0.775	0.304	0.39	2.51	0.770	2.731	0.430	0.954	0.046	0.54
PI/3	1.890	0.564	0.00	1.018	0.198	0.015	4.791	−1.7	0.726	0.293	0.40	2.77	0.769	2.761	0.487	0.924	0.076	0.70
PI/3	1.905	0.534	0.00	1.041	0.191	0.013	4.807	−1.7	0.740	0.301	0.41	2.72	0.767	2.754	0.465	0.931	0.069	0.66
PI 98/3 A	1.921	0.494	0.003	1.066	0.177	0.025	4.804	−1.8	0.764	0.302	0.40	2.66	0.767	2.745	0.435	0.941	0.059	0.58
PI 98/3 B	1.935	0.504	0.004	1.038	0.182	0.022	4.824	−1.8	0.757	0.280	0.37	2.64	0.764	2.745	0.444	0.940	0.060	0.59
PI 98/3 C	1.927	0.474	0.002	1.081	0.178	0.024	4.876	−1.9	0.774	0.307	0.40	2.53	0.756	2.733	0.426	0.952	0.048	0.54
PI 98/3 D	1.929	0.483	0.005	1.068	0.173	0.027	4.862	−1.9	0.769	0.299	0.39	2.65	0.758	2.743	0.426	0.942	0.058	0.56
mean	1.90	0.51	0.00	1.07	0.19	0.02	4.84	−1.82	0.75	0.31	0.42	2.54	0.762	2.737	0.458	0.948	0.948	0.60
s.d.[3]	0.05	0.03	0.00	0.04	0.02	0.01	0.06	0.11	0.02	0.04	0.06	0.17	0.009	0.014	0.032	0.014	0.014	0.06
PI17-h Franckeite	1.912	0.018	0.615	0.845	0.212	0.083	4.811	−1.7	0.725	0.120	0.17	2.51	0.77	2.75	0.552	0.94	0.06	0.62
PI17-d Cylindrite	1.134	0.042	0.509	0.947	0.179	0.031	4.191	−2.2	0.740	0.207	0.28	2.67	0.68	1.92	0.428	0.92	0.08	0.56

[1] valence total calculated with Sn^{2+} only, and used to adjust the Sn^{4+}/Sn^{2+} ratio
[2] CT (charge transfer): excess of positive charges in the *Q* layer, equilibrated by its deficit in the *H* layer
[3] standard deviation

atoms substituting for two Pb^{2+} atoms in the *Q* layer. In the *H* layer, the percentage of Fe^{2+} substituting for Sn^{4+} varies from 17 to 25 at.%. In franckeite (Bernhardt, 1984), this percentage is significantly higher, and varies from 28 to 34 at.%; but at Pirquitas, the franckeite variation is only 21 at.% (Table 5*b*).

Figure 12 shows As/Fe as a function of Fe content. As indicated above for analyses of type coiraite, this ratio always exceeds 2 (2.2−2.8). A small fraction of As^{3+} is sometimes compensated by minor Ag^{+}, with (As^{3+} + Ag^{+}) substituting for 2 Pb^{2+} in the *Q* layer. However, if all As is assigned to the *Q* layer and all Fe to the *H* layer there is an excess of positive charge in the *Q* layer relative to the negative charge in the *H* layer. To balance the formula, it is necessary to divide this excess of positive charge into two parts – As in both the *Q* and *H* layer, which then produces the general formula for a total of 22 *Me* atoms as:

$$[(Pb_{16-x-2y-z}Sn_xAs_{2y+z})S_{16}]\cdot[(Sn_{6-y-z}Fe_yAs_z)S_{12}]$$

Thus, substitution of *z* As^{3+} for *z* Pb^{2+} is compensated by *z* As^{3+} substituting for *z* Sn^{4+}, according to the heterovalent substitution rule: Pb^{2+} + Sn^{4+} → 2 As^{3+}. According to Table 5*b*, *z* varies from 0.12 to 0.48, and the mean analysis gives the formula:

$$[(Pb_{11.28}Sn_{1.91}As_{2.72}Ag_{0.12})_{\Sigma=16}S_{16}]\cdot [(Sn_{4.8}Fe_{1.1}As_{0.3})_{\Sigma=6}S_{12}]$$

Electron microprobe analyses (*n* = 27) of franckeite reported by Bernhardt (1984) have an Sb/Fe atomic ratio (after subtracting some Sb according to the rule Sb^{3+} + Ag^{+} → 2 Pb^{2+}) of between 1.80−2.33. Very few of these analyses indicate an Sb excess relative to Fe. At Pirquitas, the Sb/Fe atomic ratios of franckeite and cylindrite are 2.52 and 2.67, respectively, clearly indicating that there is a definite Sb excess. Our data suggest the possible incorporation of a minor amount of As or Sb into the *H* sub-layer of franckeite-type minerals. Such a substitution was first proposed by Makovicky (1974) for Sb in the *H* sub-layer of the parent homologue cylindrite. Similarly, a (Bi + Sb) excess over (½Cu + Fe) was observed amongst some synthetic members of the cylindrite-levyclaudite solid solution (Evain *et al.*, 2006).

Sn^{2+} vs. Sn^{4+}

While Sn is present in the *H* layer exclusively as Sn^{4+}, some Sn^{2+} may be incorporated in the *Q* layer substituting for Pb^{2+} (Bernhardt, 1984; Amthauer, 1986) (Table 5*b*; Fig. 13). On the basis of a total of 3.69 *Me* atoms, calculated Sn^{2+} varies from 0.28 up to 0.34 atoms; corresponding to 8−13 at.% substitution within the *Q* layer. Franckeite has lower Sn^{2+} contents (~4 at.% substitution) than coiraite, while for cylindrite one analysis gives 11 at.% substitution.

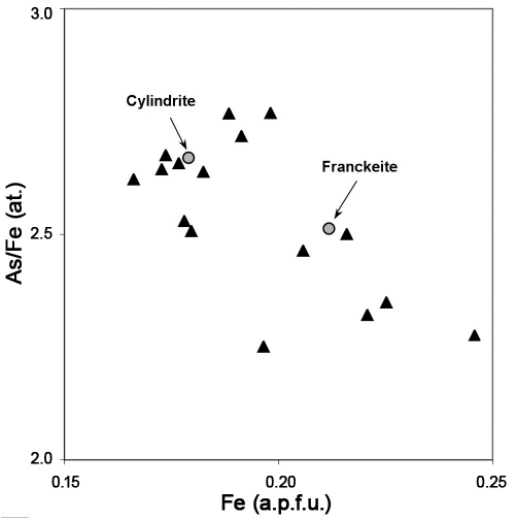

FIG. 12. Correlation between the (As – Ag)/Fe atomic ratio and the Fe content (a.p.f.u.) in coiraite, and also the (Sb–Ag)/Fe atomic ratio and Fe (a.p.f.u.) for the associated cylindrite and franckeite.

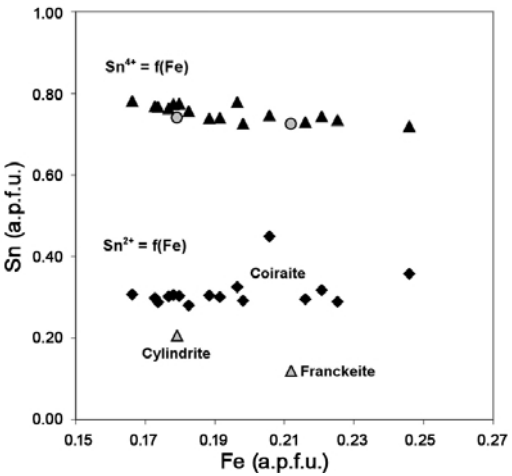

FIG. 13. Correlation between Sn and Fe (a.p.f.u.) in coiraite, associated cylindrite and franckeite. Sn^{4+} and Sn^{2+} correspond to Sn in the *H* and *Q* layers, respectively.

Coiraite synthesis

At an early stage of the current work, preparation of specimens containing synthetic 'arseno-franckeite' was envisaged by two of us (WHP and CJS). Multiphase samples of the Pb-Sn-Fe-As-S system with $Pb_{5.6}Sn_{3.1}Fe_{0.6}As_{1.5}S_{14}$ as the starting composition were then prepared by melt synthesis starting from element mixtures. Electron microprobe analyses of polished sections from the reguli (Topa 1999, unpublished) revealed strong As-deficiency and inhomogeneous chemistry of the 'arseno-franckeite'-related major phase, compared to the natural material. Variation of input composition only allowed for minor improvement in this composition. Work on polymetallic sulphide (telluride) liquids in nagyágite and buckhornite melt synthesis (Effenberger *et al.*, 1999, 2000), where Ag-doping turned out to be favourable for fractional crystallization, suggested that we focus on the Ag-Pb-Sn-Fe-As-S system. Silver is abundant at Pirquitas and is a non-essential franckeite constituent (Li, 1984, 1986). Systematic approximation towards compositional homogeneity and As-enrichment of the 'arseno-franckeite'-like phase finally yielded the current synthesis route.

The analytical or higher-grade reagents Ag_2S (Fluka), Pb (BMG), Sn (Fluka), Fe powder (Fluka), As (Aldrich) and S (Fluka), in portions according to the formula $Ag_{0.4}Pb_{5.6}Sn_{2.7}Fe_{0.6}As_{2.1}S_{14.2}$ (1.2 g total sample mass), were sealed in Duran® glass ampullae 10/2.2 at 0.1 bar N_2 atmosphere. One ampulla per synthesis run, vertically positioned in a Naber Labotherm furnace, was then heated to 480ºC at a rate of 4 K/min and kept there for 24 h. After further heating at the chosen rate, a second pre-reaction step at 580ºC (20 h) followed. The heating program was then continued and finished at 780ºC (15 min). Superheating of the melt to 780ºC (820ºC in a few cases), as homogeneity was not satisfactory achieved at 740ºC, was done to promote Fe distribution over the sample volume. Finally, the ampulla was cooled down to room temperature within 22 h inside the furnace. A vertical temperature gradient of ~1 K/cm was attained by using a fireclay thermal load-ground plate (at some distance from the ampulla bottom) inside, combined with keeping the end of the Duran® tube (at furnace insulation diameter plus a few centimetres above the top of the sealed ampulla part) outside the furnace.

The resulting surfaces of the reguli have a metallic lustre and show numerous craters, in some of which were small crystals. Inside, there were larger cavities filled with crystal aggregates up to 2 mm in size. Electron microprobe analysis gave 3.8–4.7 wt.% As in the 'arseno-franckeite'-like main phase, the As-rich end data corresponding to an approximate $Ag_{0.03}Pb_{5.5}Sn_{3.2}Fe_{0.7}As_{1.3}S_{14}$ chemical composition (or $(Ag_{0.06}Pb_{11}Sn_{1.4})_{\Sigma=12.46}As_{2.6}Sn_5Fe_{1.4}S_{28}$, written in terms of the idealized coiraite formula). Galena was present as a major constituent of the minority/impurity phases.

Conditions of formation

Coiraite and the commonly associated suredaite are known only from the Ag-Sn deposits of Pirquitas, particularly in the Oploca sector. Both minerals are abundant and thus constitute economically significant tin ores. The conditions of formation for both minerals are difficult to determine. The temperature of formation for coiraite was probably low, as indicated by the frequently colloidal texture of the ore layers. Fe in coiraite is divalent and favoured by a relatively low f_{S_2}. However, trivalent As needs a relatively high f_{S_2}. According to thermochemical data, these two constraints can be related to the pyrite-pyrrhotite equilibrium (log f_{S_2} ~−14; Toulmin and Barton, 1964) and the orpiment-realgar equilibrium (log f_{S_2} ~−12; Barton and Skinner, 1979), respectively.

The sulphur for coiraite and suredaite probably resulted from leaching of early-stage pyrite and marcasite, which are the dominant sulphides in the deposit. The source of the As could have been either arsenopyrite (a widespread constituent in the ores) and/or native As, the latter present in a few veins exposed in the recently constructed ramp. Coiraite crystallized after suredaite. The earlier crystallization of suredaite, where Sn is essentially present as SnS_2 indicates the highest f_{S_2}, while Sn in coiraite is partly present as SnS and SnS_2, pointing toward a decrease of f_{S_2}. Nevertheless, the abundant formation of coiraite and suredaite remains a geochemical anomaly. Similar prerequisites for the formation of coiraite-suredaite prevail in many of the Ag-Sn deposits of Bolivia (Ahlfeld and Schneider-Scherbina, 1964), but neither is known to occur elsewhere.

Acknowledgements

WHP is grateful to the Austrian Research Council (FWF) which supported field and laboratory work

in Argentina and Austria through grants P 11987 and 13947. The authors thank the Austrian Academy of Sciences ('Kommission für Grundlagen der Mineralrohstoffforschung') for granting two projects in 2006 and 2007 which allowed them to undertake detailed underground research at the Oploca sector of Pirquitas. They also appreciated the help, generous support and hospitality of Guillermo Gimeno, Managing Director of Sunshine Argentina, Inc. and Mario Tonel, senior exploration geologist of this company, and to Silver Standard Resources, Inc., the current owner of the property, especially to Eng. Fortunato Ramirez Cortes, Managing Director, and Victor Vaca, chief geologist. WHP also thanks Prof. Fritz Ebner, Mining University of Leoben, Austria, and his former students Gerhard Amann, Klaus Robl, Hubert Putz, Johannes Horner and Florian Albrecht for help and support during numerous stays at Pirquitas during the last fifteen years. The help of Irina Naumova with the calculation of the standard deviations is appreciated. We thank Prof. Frank Hawthorne and an anonymous reviewer for critical comments and stylistic amendments, all of which helped to improve the manuscript considerably. Our thanks also go to Dr M.D. Welch, Principal Editor and to Dr Elena Sokolova, Associate Editor, for their efforts and support. The current project on coiraite benefited from the long-standing, close cooperation of KELAG – Kärntner Elektrizitäts-Aktiengesellschaft, Klagenfurt, and the Department of Materials Engineering and Physics, Division of Mineralogy, University of Salzburg. FJC thanks DI. Dr Michael M. Marketz for excellent RD&D coordination and Mr Josef Sitter for technical assistance.

References

Ahlfeld, F. and Schneider-Scherbina, A. (1964) Los yacimientos minerales y de hidrocarbu-ros de Bolivia. *Departamento Nacional de Geología, La Paz, Bolivia, Boletin Especial*, **5**.

Amann, G. and Paar, W.H. (2001) Structural control of Ag-Sn Vein-Type Mineralisation at the Pirquitas Mine (Prov. Jujuy, NW-Argentina) – Ore Precipitation during Fold and Thrust Belt Evolution. *EUG XI*, Abstract Volume **6/1**, 266.

Amthauer, G. (1986) Crystal chemistry and valencies of iron, antimony, and tin in franckeites. *Neues Jahrbuch für Mineralogie Abhandlungen*, **153**, 245–324.

Barton, P.B. and Skinner, B.J. (1979) Sulfide mineral stabilities. Pp. 278–403 in: *Geochemistry of Hydrothermal Ore Deposits* (H.L. Barnes, editor). 2nd edition, Wiley, New-York. 798 pp.

Bernhardt, H.-J. (1984) The composition of natural franckeites. *Neues Jahrbuch für Mineralogie Abhandlungen*, **150**, 25–64.

Coira, B.L. and de Brodtkorb, M.K. (1995) Polymetallic mineralization associated with Cenozoic volcanism in Northern Puna, Argentina. *Pacrim* '**95**, 135–140.

Cordier, G. and Schäfer, H. (1981) $Ca_2Sb_2S_5$, ein neues Erdalkalithioantimonat (III) mit Sb_2S_4-Viererringen. *Revue de Chimie Minérale*, **18**, 218–223.

Criddle, A.J. and Stanley, C.J. (1993) *The Quantitative Data File for Ore Minerals*. The Commission on Ore Mineralogy, International Mineralogical Association. Chapman & Hall, London, UK.

Effenberger, H., Paar, W.H., Topa, D., Culetto, F.J. and Giester, G. (1999) Toward the crystal structure of nagyágite, $[Pb(Pb,Sb)S_2][(Au,Te)]$. *American Mineralogist*, **84**, 669–676.

Effenberger, H., Culetto, F.J., Topa, D. and Paar, W.H. (2000) The crystal structure of synthetic buckhornite, $[Pb_2BiS_3][AuTe_2]$. *Zeitschrift für Kristallographie*, **215**, 10–16.

Ericksen, G.E. and Cunningham, C.G. (1993) *Precious-metal deposits in the Neogene-Quaternary volcanic complex of the Central Andes*. Investigación de metales preciosos en los Andes Centrales. Proyecto BID/TC-88-02-35-5, 3–16.

Evain, M., Petříček, V., Moëlo, Y. and Maurel, C. (2006) First (3+2)-dimensional superspace approach of the structure of lévyclaudite-(Sb), a member of the cylindrite-type minerals. *Acta Crystallographica*, **B62**, 775–789.

Lafond, A., Nader, A., Moëlo, Y., Meerschaut, A., Briggs, A., Perrin, S., Monceau, P. and Rouxel, J. (1997) X-ray structure determination and superconductivity of a new layered misfit compound with a franckeite-like stacking, $[(Pb,Sb)S]_{2.28}NbS_2$. *Journal of Alloys and Compounds*, **261**, 114–122.

Li, J. (1984) Franckeite syntheses and heating experiments. *Neues Jahrbuch für Mineralogie Abhandlungen*, **150**, 45–50.

Li, J. (1986) Cylindrite syntheses and relations to franckeite. *Neues Jahrbuch für Mineralogie Abhandlungen*, **153**, 283–285.

Makovicky, E. (1974) Mineralogical data on cylindrite and incaite. *Neues Jahrbuch für Mineralogie Monatshefte*, 235–256.

Makovicky, E. and Hyde, B.G. (1992) Incommensurate, two-layer structures with complex crystal chemistry: Minerals and related synthetics. *Materials Science Forum*, **100** and **101**, 1–100.

Makovicky, E., Petříček, V., Duček, M. and Topa, D. (2008) Crystal structure of a synthetic tin-selenium

cylindrite. *American Mineralogist*, **93**, 1787–1798.

Malvicini, L. (1978) Las vetas de estaño y plata de mina Pirquitas (Pircas), prov.de Jujuy, Republica Argentina. *Revista de la Asociación Argentina de Mineralogía, Petrología y Sedimentología, Rev.* **9**, 1–26.

Meerschaut, A., Moëlo, Y., Cario, L., Lafond, A. and Deudon, C. (2000) Charge transfer in misfit layer chalcogenides, $[(MX)_n]_{1+x}(TX_2)_m$: A key for understanding their stability and properties. *Molecular Crystals and Liquid Crystals*, **341**, 1–8.

Moëlo, Y., Makovicky, E., Mozgova, N.N., Jambor, J.L., Cook, N., Pring., A., Paar, W.H., Nickel, E.H., Graeser, S., Karup-Møller, S., Balic-Zunic, T., Mumme, W.G., Vurro, F., Topa, D., Bindi, L., Bente, K. and Shimizu, M. (2008) Sulphosalt systematics: a review. Report of the sulphosalt subcommittee of the IMA Commission on Ore Mineralogy. *European Journal Mineralogy*, **20**, 7–46.

Mottana, A., Fiori S. and Parodi, G.C. (1992) Improved X-ray powder diffraction data for franckeite. *Powder Diffraction*, **7**, 112 (PDF No 43-1480).

Organova, N.I. (1989) Crystallochemistry of incommensurate and modulated mixed-layer minerals. Moscow, Nauka, **144** (In Russian).

Paar, W.H., de Brodtkorb, M.K., Topa, D. and Sureda, R.J. (1996) Caracterización mineralógica y química de algunas especies metalíferas de yacimiento Pirquitas, Provincia de Jujuy, República Argentina: Parte 1. XIII Congreso Geológico y III Congreso de Exploracíon de Hidrocarburos, *Actas III*, 159–172.

Paar, W.H., de Brodtkorb, M.K., Sureda, R.J. and Topa, D. (1998) A microprobe study of complex Ag-Sn ores from Pirquitas, Jujuy Province, Argentina. *17th General Meeting of the International Mineralogical Association, Toronto, Canada. Abstract Volume*, p. A 118.

Paar, W.H., Miletich, R., Topa, D., Criddle, A.J., de Brodtkorb, M.K., Amthauer, G. and Tippelt, G. (2000) Suredaite, $PbSnS_3$, a new mineral species, from the Pirquitas Ag-Sn deposit, NW-Argentina: Mineralogy and Crystal Structure. *American Mineral*ogist, **85**, 1066–1075.

Paar, W.H., de Brodtkorb, M.K., Sureda, R.J. and Topa, D. (2001) Mineralogía y quimismo de sulphuros y sulfosales de estaño y plomo en las vetas de Mina Pirquitas, Jujuy, Argentina (22º41'S – 66º28'W). *Revista Geologica de Chile*, **28**, 259–268.

Paar, W.H., Putz, H., Topa, D., Sureda, R.J., de Brodtkorb, M.K. and Lüders, V. (2006*a*) Breccias with high-grade Ag-Sn mineralization at Pirquitas, Argentina. *19th General Meeting of the International Mineralogical Association, Kobe, Japan. Abstract Volume*, p. 193.

Paar, W.H., Putz, H., Sureda, R.J., Ebner, F. and Iradi, P. (2006*b*) Ore deposit mineralogy of high-grade silver-tin-zinc mineralization at the Oploca vein- and breccias system, Pirquitas, province of Jujuy, Argentina. *Unpublished report*, 18 pp.

Shimizu, M., Moh, G.H. and Kato, A. (1992) Potosiite and incaite from the Hoei Mine, Japan. *Mineralogy and Petrology*, **46**, 155–161.

Sillitoe, R.H., Steele, G.B., Thompson, J.F.H. and Lang, J.R. (1998) Advanced argillic lithocaps in the Bolivian tin-silver belt. *Mineralium Deposita*, **33**, 539–546.

Sureda, R.J., Galliski, M.A., Argañaraz, P. and Daroca, J. (1986) Aspectos metalogénicos del noroeste argentino (provincias Salta y Jujuy). *Capricornio*, **1**, 39–96.

Toulmin, P. and Barton, P.B. (1964) A thermodynamic study of pyrite and pyrrhotite. *Geochimica Cosmochimica Acta*, **28**, 641–671.

Wiegers, G.A. and Meerschaut, A. (1992) Misfit layer compounds $(MS)_nTS_2$ (M = Sn, Pb, Bi, Rare Earth metals; T = Nb, Ta, Ti, V, Cr; $1.08 < n < 1.23$): Structures and physical properties. *Materials Science Forum*, **100** and **101**, 101–172.

Williams, T.B. and Hyde, B.G. (1988) Electron microscopy of cylindrite and franckeite. *Physics and Chemistry of Minerals*, **15**, 521–544.

Williams, T.B. and Pring, A. (1988) Structure of lengenbachite: A high-resolution transmission electron microscope study. *American Mineralogist*, **73**, 1426–1433.

Wolf, M., Hunger, H.-J. and Bewilogua, K. (1981) Potosiit - ein neues Mineral der Kylindrit-Franckeit-Gruppe. *Freiberger Forschungshefte*, **C 364**, 113–133.